

Electrically controlled negative refraction in a nematic liquid crystal

Oleg P. Pishnyak^{a)} and Oleg D. Lavrentovich^{b)}

Liquid Crystal Institute and Chemical Physics Interdisciplinary Program, Kent State University, Kent, Ohio 44242

(Received 7 September 2006; accepted 11 November 2006; published online 18 December 2006)

The authors demonstrate electrically controlled negative refraction at the interface between an isotropic material and a uniaxial nematic liquid crystal, in which the optic axis is designed to make a large angle with the interface. Depending on the applied voltage, the refracted beam is either on the opposite side of the interface normal as compared to the incident beam (positive refraction) or on the same side (negative refraction). © 2006 American Institute of Physics.

[DOI: 10.1063/1.2408658]

Refraction is said to be negative when, on passing through an interface between two media, the tangential component of the time-averaged Poynting vector changes its sign, i.e., the incident and the refracted rays are on the same side of the surface normal.¹ Negative refraction can be observed for an interface between a normal material and a so-called left-handed material (LHM), in which the electric permittivity and magnetic permeability are both negative. A flat LHM slab can perform as a “superlens” with subwavelength resolution.² Although LHMs can be constructed for infrared and microwave ranges, the current LHM designs are not yet practical for the visible spectrum. Much of the research is thus directed to analyze whether and how the conventional materials with positive refractive index n can be designed to mimic some features of LHMs.¹ It was found, surprisingly not a long time ago, that negative refraction occurs in normal positive index media, namely, birefringent solid crystals such as YVO₄.^{3–6} The physics is that the directions of wave and energy propagation for the extraordinary mode in birefringent medium do not coincide. To the best of our knowledge, the phenomenon was not demonstrated so far for the liquid crystals (LCs); the advantage over the solid crystals is that light propagation can be easily controlled by electric field that changes the optic axis (the director \mathbf{n}) orientation. In this work, by employing a special cell design that sets a large ($\sim 45^\circ$) tilt of \mathbf{n} at the front interface, we demonstrate that the negative refraction does exist in a uniaxial nematic LC and that it can be switched to the positive refraction by an applied electric field.

A planar interface $z=0$ separates an isotropic medium of a refractive index $n_i \geq 1$ occupying the half-space $z < 0$ from a nematic LC with the ordinary index n_o and the extraordinary index $n_e > n_o$ at $z > 0$. The optic axis (\mathbf{n}) is in the plane x - z , making an angle α with the z axis, Fig. 1. Consider a plane wave, linearly polarized in the x - z plane; the incident angle in the isotropic phase is θ_i . The dispersion equation for the normalized components of the wave vector found from Maxwell’s equations reads in the isotropic medium as

$$k_{ix}^2 + k_{iz}^2 = n_i^2, \tag{1}$$

and in the LC as

$$ak_{ix}^2 + bk_{iz}^2 + ck_{ix}k_{iz} = 1 \tag{2}$$

where $a = n_o^{-2} \sin^2 \alpha + n_e^{-2} \cos^2 \alpha$, $b = n_o^{-2} \cos^2 \alpha + n_e^{-2} \sin^2 \alpha$, $c = \sin 2\alpha (n_e^{-2} - n_o^{-2})$, and the components of the transmitted wave vector \mathbf{k}_t define the angle $\theta_{t,k} = \tan^{-1}(k_{tx}/k_{tz})$, see Ref. 7. The direction of the refracted time-averaged Poynting vector \mathbf{S}_r , characterized by the angle $\theta_{r,S} = \tan^{-1}(S_{rx}/S_{rz})$ that \mathbf{S}_r makes with the z axis, is perpendicular to the \mathbf{k}_t surface, and at any point (k_{tx}, k_{tz}) it is found from the equation $\tan \theta_{r,S} = (\partial \varphi / \partial k_{tx}) / (\partial \varphi / \partial k_{tz})$, where $\varphi(k_{tx}, k_{tz}) = ak_{ix}^2 + bk_{iz}^2 + ck_{ix}k_{iz}$, Fig. 1. Using the boundary condition $k_{ix} = k_{tx}$ at $z=0$ and expressing k_{iz} through k_{ix} , Eq. (2), one finds

$$\theta_{t,k} = \tan^{-1} \frac{2bn_in_on_e \sin \theta_i}{2\sqrt{bn_o^2n_e^2 - n_i^2 \sin^2 \theta_i} - cn_in_on_e \sin \theta_i}, \tag{3}$$

$$\theta_{r,S} = \tan^{-1} \frac{2n_i \sin \theta_i + cn_on_e \sqrt{bn_o^2n_e^2 - n_i^2 \sin^2 \theta_i}}{2bn_on_e \sqrt{bn_o^2n_e^2 - n_i^2 \sin^2 \theta_i}}, \tag{4}$$

the same results as those obtained by Luo *et al.*⁶ in a somewhat different way. If $\theta_i=0$, then $\theta_{t,k}=0$; a small increase $\theta_i > 0$ makes $\theta_{t,k} > 0$, too. The behavior of $\theta_{r,S}$ is different:

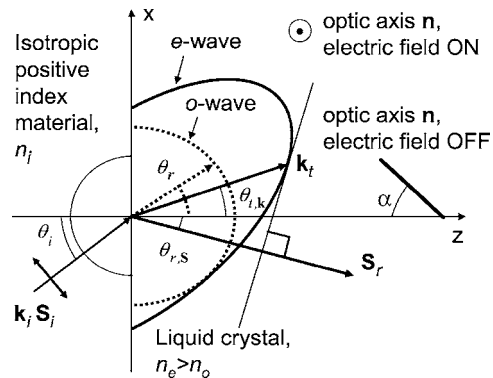


FIG. 1. Voltage-controlled amphoteric refraction at the isotropic-uniaxial nematic interface. The incident beam is polarized in the plane of figure. The wave-vector surfaces are shown as a solid circle for the isotropic medium, as a solid ellipse for the extraordinary wave, and as a dashed circle for the ordinary wave in the nematic LC. In the regime of negative refraction, no voltage is applied, and the optic axis \mathbf{n} is in the plane of figure, making a large angle α with the z axis. The energy flow direction \mathbf{S}_r in the LC is perpendicular to the ellipse at point \mathbf{k}_t and is thus different from the direction of \mathbf{k}_t . When the voltage is applied, \mathbf{n} reorients along the y axis to establish positive refraction: both the wave vector and energy flow are along the dashed vector.

^{a)}Electronic mail: opp@lci.kent.edu

^{b)}Electronic mail: odl@lci.kent.edu

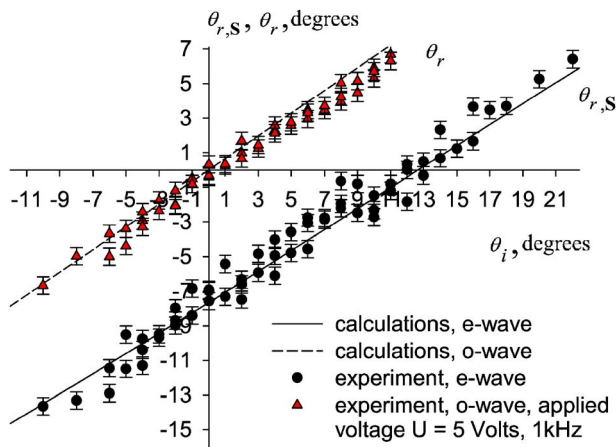


FIG. 2. (Color online) Theoretical and experimental data for the electrically controlled amphoteric refraction in E7. The extraordinary regime dependency $\theta_{r,S}(\theta_i)$, Eq. (4), is shown by the solid line and the ordinary regime dependency $\theta_r(\theta_i)$, Eq. (5), by the dashed line. In the extraordinary case, $U=0$; negative refraction is observed for $0^\circ < \theta_i < 12.5^\circ$. In the ordinary case, $U=5$ V (at 1 kHz).

for $\theta_i=0$, it can be negative, provided $\alpha \neq 0, \pi/2$, as $\theta_{r,S}(\theta_i=0) = -\tan^{-1}[(n_e^2 - n_o^2) \sin \alpha \cos \alpha / (n_o^2 \sin^2 \alpha + n_e^2 \cos^2 \alpha)]$. The solid line in Fig. 2 shows the dependence $\theta_{r,S}(\theta_i)$ as calculated from Eq. (4) with $n_i=1$, $\alpha=45^\circ$, and $n_o=1.52$ and $n_e=1.74$ (both at 633 nm), characteristic of the nematic mixture E7 (EM Industries) used in our experiments. As clear from Fig. 2 and Eq. (4), there is a range of the incident angles, $0 < \theta_i < \theta_{ic}$, where $\theta_{ic} \approx 12.5^\circ$, for which refraction is negative. The maximum (negative) angle of refraction $\theta_{r,S}^{\max} = -\tan^{-1}[(n_e^2 - n_o^2) / 2n_o n_e] = -7.7^\circ$ is achieved when $\theta_i=0$ and $\alpha = \tan^{-1}(n_e/n_o) \approx 49^\circ$.

When \mathbf{n} is turned parallel to the y axis, Fig. 1, the regime is ordinary. The wave vector and the ray vector would propagate at the same angle $\theta_r(\theta_i)$ defined from

$$n_i \sin \theta_i = n_o \sin \theta_r, \tag{5}$$

Fig. 2 (the dashed line). Therefore, by applying the electric field to the LC cell and reorienting \mathbf{n} , one can switch between negative and positive refractions.

The experimental setup is shown in Fig. 3. The He-Ne laser beam ($\lambda=633$ nm) passes through a polarizer P to achieve linear polarization in the x - z plane and is focused by a $10\times$ microscope objective O to couple it into the middle of a cell filled with E7. The diameter of the focused spot is $\sim 10 \mu\text{m}$ so that the beam intensity is $\sim 5 \text{ W/cm}^2$. This intensity is well below the one that causes significant optically induced torques on \mathbf{n} in the generation of the solitonlike formations, the so-called nematicons.^{8,9}

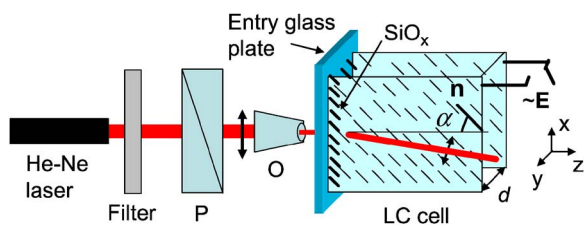


FIG. 3. (Color online) Experimental setup. The SiO_x coated glass plate is the entry plate for the laser beam. At zero voltage, the director \mathbf{n} is in the x - z plane. The electric field \mathbf{E} serves to reorient \mathbf{n} along the y axis.

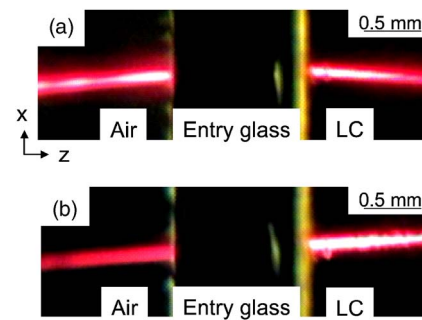


FIG. 4. (Color online) Photographs of voltage-controlled amphoteric refraction of a laser beam linearly polarized in the plane of figure, on passing through air into the entry glass plate, $\theta_i \approx 5.5^\circ$, and then into the LC. At zero voltage, refraction is negative, $\theta_{r,S} \approx -4.2^\circ$ (a); at $U=5$ V, it switches into the positive one, $\theta_r \approx 3.8^\circ$ (b).

Propagation of the beam is monitored using a charge-coupled device camera facing the x - z plane of the cell through a microscope objective. The LC cell of thickness $d=90 \mu\text{m}$ is assembled using two glass substrates with conductive indium tin oxide layers. The substrates are coated with a polyimide PI2555 (Microsystems) film rubbed to align \mathbf{n} uniformly parallel to the x - z plane but under the angle $\alpha=(45 \pm 1)^\circ$, to the z axis (Fig. 1). The third glass plate of crucial importance was an entry glass plate perpendicular to the first two. This plate imposes a highly tilted, $\alpha=(45 \pm 5)^\circ$, orientation of \mathbf{n} at the entry interface [achieved by an obliquely deposited layer of SiO_x (Ref. 10)], thus simultaneously preserving the uniformity of \mathbf{n} throughout the entire cell, Fig. 3. The LC cell can be rotated around the y axis to control θ_i .

The experimental data $\theta_{r,S}(\theta_i)$ and $\theta_r(\theta_i)$ are in good agreement with the behavior predicted by Eqs. (4) and (5), respectively, Fig. 2. Negative refraction occurs for a wide range of the incident angles, $0 < \theta_i < 12.5^\circ$, when there is no field, Figs. 2 and 4(a). The maximum (negative) bend angle is $\theta_{r,S} \approx -8^\circ$, as in the theory. By applying the electric field and reorienting \mathbf{n} along the y axis, one switches negative refraction to positive one, Figs. 2 and 4(b). We deliberately used low voltages ($U=5$ V) to demonstrate the efficiency of the control; for $d=90 \mu\text{m}$ and $U=5$ V, the angle between \mathbf{n} and the y axis is less than 2° within the central portion (of width $\approx 25 \mu\text{m}$) of the LC cell, as established by numerical simulations of the dielectric response of E7. Some deviations of the experimental $\theta_r(\theta_i)$ from Eq. (5), noticeable at large θ_i , Fig. 2, are caused by the finite width of the region with realigned \mathbf{n} ; as the beam gets defocused in the LC, it propagates in the regions where \mathbf{n} deviates from the y axis. Of course, a higher voltage would reorient a larger portion of the nematic cell and thus would refine the ordinary regime, as observed.

To conclude, we used one of the simplest possible geometries to prove the very existence of negative refraction and electrically controlled amphoteric refraction in LCs that can be used in a variety of applications, e.g., beam steering. In our cells with a large d , the characteristic time of director reorientation was tens of seconds. However, there is no principal obstacle to speed the response up by reducing d , by using dual-frequency materials or higher voltages. The biggest advantage of LCs is in the flexibility and controllability

of the optical axis \mathbf{n} . Even higher degree of flexibility is expected when the LC is used as one of the components in heterogeneous materials, in which one might hope to expand beyond the regime of negative refraction in the positive index anisotropic material presented in this work.

One of the authors (O.D.L.) thanks N. Kotov, E. E. Narimanov, V. M. Shalaev and P. Palffy-Muhoray for stimulating discussions about negative index materials. The authors thank A. Golovin for the help in experiments. The work was partially supported by NSF DMR 0504516 and MURI (AFOSR) grant FA9550-06-1-0337 on negative index materials.

- ¹Y. Zhang and A. Mascarenhas, *Mod. Phys. Lett. B* **19**, 21 (2005).
- ²J. B. Pendry, *Contemp. Phys.* **45**, 191 (2004).
- ³Y. Zhang, B. Fluegel, and A. Mascarenhas, *Phys. Rev. Lett.* **91**, 157404 (2003).
- ⁴Z. Liu, Z. Lin, and S. T. Chui, *Phys. Rev. B* **69**, 115402 (2004).
- ⁵X. L. Chen, M. He, Y. X. Du, W. Y. Wang, and D. F. Zhang, *Phys. Rev. B* **72**, 113111 (2005).
- ⁶H. Luo, W. Hu, X. Yi, H. Liu, and J. Zhu, *Opt. Commun.* **254**, 353 (2005).
- ⁷G. R. Fowles, *Introduction to Modern Optics*, 2nd ed. (Dover, New York, 1989), p. 328.
- ⁸J. Beeckman, K. Neyts, X. Hutsebaut, C. Cambournac, and M. Haelterman, *Opt. Quantum Electron.* **37**, 95 (2005).
- ⁹A. Alberucci, M. Peccianti, G. Assanto, G. Coschignano, A. De Luca, and C. Umeton, *Opt. Lett.* **30**, 1381 (2005).
- ¹⁰A. B. Golovin, S. V. Shiyankovskii, and O. D. Lavrentovich, *Appl. Phys. Lett.* **83**, 3864 (2003).